Laser Review

Towards Visible Frequency Comb Generation Using a Hollow WGM Resonator

Sho KASUMIE, Yong YANG, Jonathan M. WARD, and Síle NIC CHORMAIC

Light-Matter Interactions Unit, Okinawa Institute of Science and Technology Graduate University, Onna, Okinawa 904-0495

(Received September 8, 2017)

Optical frequency combs are widely used for metrology, optical clocks, optical communications and sensors. In whispering gallery mode (WGM) microcavity resonators, geometrical features enable the four-wave mixing phase match condition to be satisfied. Hence, frequency comb generation is achievable. Geometrical dispersion of hollow structure WGM cavities can broaden the comb span to the visible range.

Key Words: Frequency comb, Four-wave mixing, Microbubble optical resonator

1. Introduction

The ability to confine light in microscopic circular orbits by a process of continuous total internal reflection has pushed optical resonators towards the extremes of optical quality,[1] finesse[2] and mode volume.[3] These so-called whispering gallery resonators (WGRs)[4,5] and their morphological dependent resonances have found applications from ultralow threshold nonlinear optics[6,7] and lasing[8] to bio/chemical sensing,[9,10] telecommunications,[11,12] quantum optics[13] and optomechanics.[14,15] Apart from technical applications, these devices have proven to be a test bed for fundamental physics such as chaos theory[16] and quantum mechanics.[17] Frequency comb generation is arguably one of the most important applications of WGRs. Frequency combs generated by phase-locked pulsed lasers produce equidistant optical lines (or teeth) that can span from the UV to the IR.[18,19] The teeth act as an optical ruler and have greatly advanced the field of optical metrology.[20,21] Currently, optical combs require large lasers that consume a lot of power, so significant effort is being made to develop robust chip scale devices - WGRs are at the forefront of this development. In a silica WGR, a four-wave mixing (FWM) process is employed to produce the frequency comb[22,23] where the signal and idler photons are generated by the pump beam both of which are resonant with WGMs of the cavity. This is particularly challenging because the free spectral range of a WGR is not constant. In 2007, a pioneering approach for WGR comb generation was proposed and experimentally confirmed.[23] It was shown that a strong pump laser can introduce phase modulations which shift resonance modes so that the total dispersion of the cavity is in the anomalous regime, thus making the FWM process possible.[23]

Today it is possible to have on-chip WGRs, that use continuous low power pump lasers to produce stable, octave spanning IR frequency combs.[24] However, extending these devices into the visible and UV regions is technically challenging due to limitations in engineering the dispersion in the resonator. While the material dispersion is fixed, geometrical dispersion can be modified so that the total dispersion meets the required condition. In such a context, WGRs with a hollow structure and bottle shape were found to have additional degrees of freedom in their design, namely the wall thickness and curvature, which improves their geometrical dispersion manipulability.[25-28] Here, we will discuss how this dispersion engineering has been, to date, implemented in hollow WGRs to create IR and visible combs.

2. Dispersion Management in Microbubble Resonators

To achieve efficient FWM needed for generating a frequency comb, a phase matching condition is required. For WGMs, the mode structure is affected by both the material and the geometric dispersion. In total, the dispersion of a WGR can be described as the variation of the free-spectral-range ($\Delta\omega_{FSR}$) and is categorized as normal ($\Delta\omega_{FSR} < 0$) or anomalous ($\Delta\omega_{FSR} > 0$). The dispersion compensated regime is when the FSR is independent of wavelength (i.e. $\Delta\omega_{FSR} < \gamma$ and γ is the linewidth of the cavity mode). In one-dimensional resonators, such as a Fabry-Pérot cavity, the total dispersion is determined by the material which usually has normal dispersion. By introducing confinement, the total dispersion can be flattened yet still remains in the normal dispersion regime due to the overlap with air.[29] In WGRs, the confinement of the optical modes and the geometry of the resonator can be modified in three-dimensions. Changing the geometry of the WGR, and therefore the physical path of the WGMs, one can modify the effective refractive index of the modes (this is also true for different mode orders) and this is the origin of the geometric dispersion. Therefore, by carefully controlling the size of the WGR, the material dispersion can be controlled. For a microsphere whose with a diameter larger than 150 μm, at a wavelength of 1.55 μm, the resonator is in the anomalous dispersion regime. With introduction of the Kerr effect, by pumping with an appropriate laser power, the total dispersion can be compensated and degenerate FWM can be achieved.[29,30]

For microtoriods, dispersion compensation is easier to control by varying the minor diameter of the toroid.[23] Changing the diameter of the WGR only results in a slight change in the total dispersion. By altering the material[31] or choosing higher order radial and azimuthal modes in the WGR, the dispersion can also be slightly managed. This method was used for achieving mid-IR comb generation in fluoride WGRs.[32]

In order to expand comb generation, the dispersion should be more freely controlled, i.e. both the zero dispersion wavelength (ZDW) and the flatness of the dispersion curve need to be managed. According to the principle mentioned above, a synthetic dimension needs to be introduced to the 3D WGR. To-date there are three ways reported: (i) Change the lateral profile of the WGR and excite 3D confined bottle-like modes. The earliest experimental demonstration was by Savchenkov *et al.*, who observed 790 nm comb generation by exciting the lateral modes in a CaF_2 cylinder;[33] (ii) Use a wedged silica microdisk.[34] Microdisks with multiple wedges were fabricated, so that the shorter wavelength modes and longer wavelength modes occupied different space at the wedges, thus experiencing different effective refractive indices; (iii) Make a hollow structure such as a microbubble. Microbubbles can be fabricated using several techniques.[27,35,36] For example, in our earlier work,[37] two counter-propagating CO_2 laser beams were used. The main point is to heat a small section of silica capillary while pressurizing the air inside the capillary. When the glass becomes soft, the air pressure pushes out the wall of the capillary to form a bubble shape. In order to get ultrathin walls and the intended bubble diameter/shape, the capillary is first tapered using a CO_2 laser and mechanical pulling stages.

It was first proposed in 2013[26] that microbubbles could be used for comb generation. The authors pointed out that the dispersion can be altered not only by changing the diameter of the microbubble, but also by varying the wall thickness or filling the core of the microbubble with different materials. In this way, the ZDW of the WGR can be shifted towards the ZDW of silica. They designed and fabricated a microbubble with diameter of 134 μm and wall thickness of 3–4 μm.

With a pumping power of 3 mW, degenerated FWM occurred at 1.55 μm, see Fig. 1. In comparison, degenerated FWM could not be excited in a microsphere of the same diameter, which proved their claim. This work showed that the wall thickness of the microbubble provides a way to control the dispersion. Later, in 2015, Farnesi *et al.* fabricated a silica microbubble with diameter of 475 μm and wall thickness of 3–4 μm.[38] By increasing the pumping power up to 80 mW, they succeeded to obtain Type I and Type II frequency combs at a wavelength of 1.56 μm,[38] see Fig. 2. Hyperparametric oscillation incorporating FWM, a Raman process and other nonlinear effects provided a much broader bandwidth comb than the previous work.[26] These two works show the capability of silica microbubbles for IR comb generation. For comb generation in the visible spectrum, the wall thickness needs to be

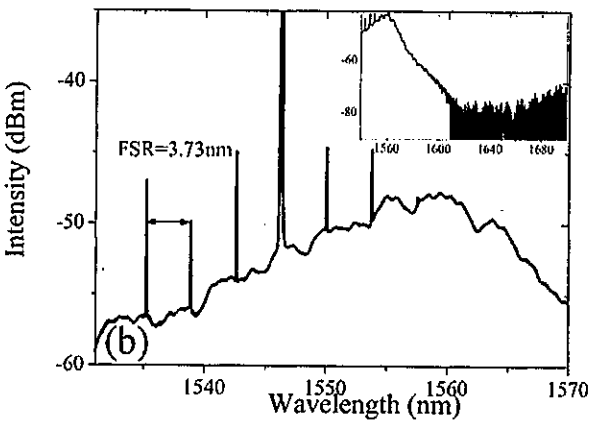

Fig. 1 Degenerate FWM in a dispersion compensated microbubble resonator. Reproduced with permission from. ref. 26)

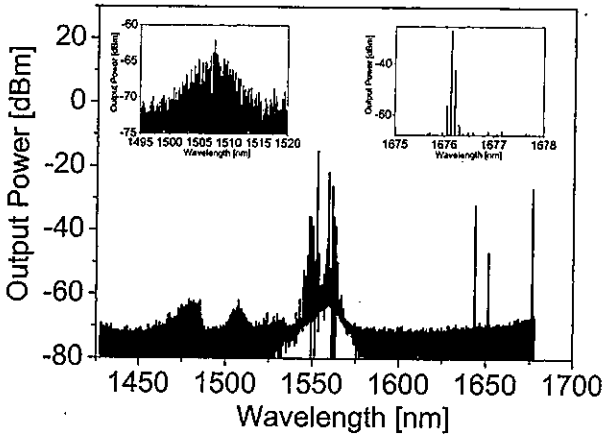

Fig. 2 Hyperparametric oscillation and IR comb generation in a microbubble resonator. Reproduced with permission from. ref. 38)

reduced further so that the ZDW of the microbubble can be shifted to even shorter wavelengths, as will be discussed in Section IV.

3. Comb Generation in Bottle-Like Microresonators

While the modes in conventional WGRs are generally confined to the equator, bottle-like microresonators (BLMRs) are unique as the optical modes expand in two dimensions along the surface and have been termed whispering gallery etalons or bottle resonators (Fig. 3). The two dimensional distribution of the optical mode also creates an equally spaced FSR. Consider a BLMR with a parabolic curvature profile along the z-axis of its cylindrical coordinate. The diameter is $R(z) = R_0[1-(\zeta z)^2/2]$, where R_0 is the maximum radius at $z = 0$ and ζ is the curvature. The eigenfrequency of the bottle modes is[25]

$$\nu_{j,m} = \frac{c}{2n\pi}\sqrt{\frac{j^2}{R_0^2}+\frac{2\zeta j}{R_0}\left(m+\frac{1}{2}\right)} \qquad (1)$$

with j and m representing its longitudinal and axial mode numbers, c and n represent the speed of light in vacuum and the refractive index in the material, respectively. In a practical system, with very small curvature, the variation of the

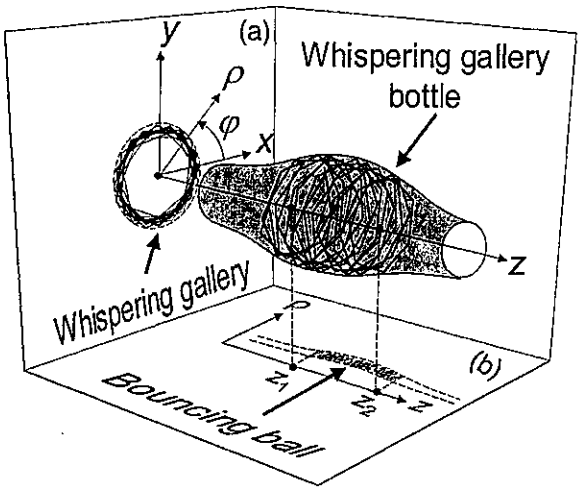

Fig. 3 Illustration of a bottle mode. Reproduced with permission from. ref. 25)

FSR is

$$\Delta\nu^{G}_{FSR} \approx \frac{c\left[\zeta R_0 (m+1/2)\right]^2}{2\pi n R_0 j^3} \quad (2)$$

The material dispersion is $\Delta\nu^{0}_{FSR} \approx c^2\lambda^2/(4\pi^2 n^3 R^2) \cdot \nu_{GVD}$ and $\nu_{GVD} = -(\lambda/c)(\partial^2 n/\partial\lambda^2)$ with λ representing the wavelength.

The dispersion curves for bottle modes and WGMs in BLMRs of radii 51 μm and 75 μm are plotted in Fig. 4 which shows that the dispersion is always in the anomalous regime around 1.55 μm regardless of the bottle's diameter.[28] It can also be seen that, for the bottle modes, geometric dispersion does not shift the ZDW significantly, while the dispersion for the WGM shifts the ZDW depending on the radius of the BLMR. In a hollow WGR, the geometric dispersion can be managed by designing the diameter, curvature and wall thickness. The implication for this is that for a conventional WGM at 1.55 μm it is not possible to create a comb in a resonator with a diameter below 150 μm due to the normal dispersion at small diameters. However, for bottle modes, anomalous dispersion can be maintained at smaller diameters due to the additional geometric dispersion of these modes.

To test this hypothesis in experiment, a BLMR with a diameter of 102 μm and a stem diameter 90 μm was fabricated. The wall thickness was estimated to be 3–4 μm and did not play any role in this case. Light was coupled to the BLMR via a tapered fibre that was mounted so that its position along the z-axis could be finely adjusted. Of course, not only the third nonlinearity FWM is excited, Raman scattering can also generate a frequency comb.[38] To exclude the Raman process, the laser power was kept above the FWM threshold but below the Raman lasing threshold. Frequency comb generation by FWM was confirmed by judicious selection of the fibre position, i.e. when a WGM was pumped no FWM was generated; however, when the tapered fiber position was moved to pump a bottle mode then FWM was observed (Fig. 5). Thus, it was shown that the dispersion can be engineered in bottle modes to lift the restrictions imposed by conventional WGMs. As stated, the wall thickness did not play a role in this experiment; however, combining the effect of the parabolic curvature with a thin wall remains to be explored as an additional means of dispersion tuning.

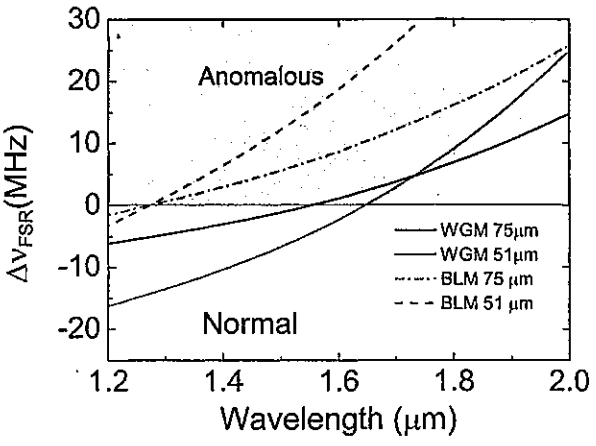

Fig. 4 Total dispersion of a BLM in terms of the FSR variation for different working wavelengths. Reproduced with permission from. ref. 28)

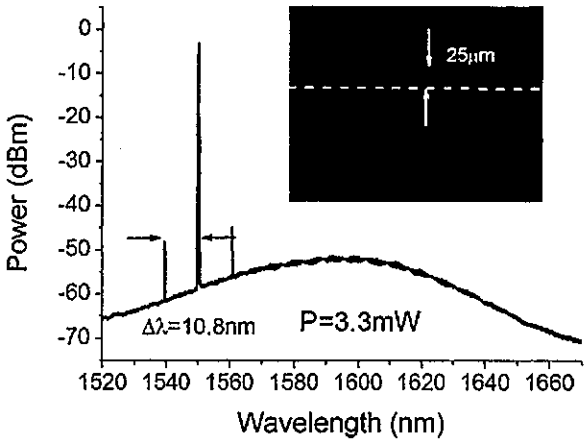

Fig. 5 FWM in a hollow BLMR when the taper is positioned 25 μm away from the center (dashed line). Reproduced with permission from. ref. 28)

4. Visible Comb Generation in Microbubble Resonators

To-date, most visible comb generation in WGRs is done indirectly. An IR comb is first generated through FWM and then is mapped to the visible range through second[39] and third harmonic generation.[40] This was demonstrated in a Si_3N_4 microring by exploiting the high nonlinearity of the material. The low effeciency of the higher order harmonic generation process results in lower quality combs, compared to direct IR Kerr combs. Thus, combs generated directly by visible frequency FWM is still being studied. As discussed in the introduction, and the previous section, direct Kerr frequency comb generation in the visible range from silica microspheres, toroids or disks is almost impossible due to the material dispersion limit. Better dispersion engineering is required to go beyond this limitation.

A route to visible combs in hollow microcavities was recently detailed theoretically[41] for a spherical bubble WGR. The inner diameter, wall thickness and outer diameter are ρ_0, t and $\rho_1 = \rho_0 + t$, respetively. For a general case, the inner medium, the bubble wall and surrounding medium can all have different refractive indices, n_1, n_2 and n_3, respectively. Then the eigenfrequency is determined by the characteristic equation

$$n_3^p \frac{X_1'(z_{31})}{X_1(z_{31})} = n_2^p \frac{N_1\psi_1'(z_{21}) + X_1'(z_{21})}{N_1\psi_1(z_{21}) + X_1(z_{21})} \quad (3)$$

where $z_{ij} = kn_i\rho_j$, k is the complex wavenumber and l is the azimuthal mode number. For simplicity, k is real $k = 2\pi/\lambda$ and only the first order radial mode is considered. $p = \pm 1$ is the polarization coefficient where $p = 1$ for TE modes and $p = -1$ for TM modes and the coefficient N_1 is

$$N_1 = \frac{n_1^p\psi_1'(z_{10})X_1(z_{20}) - n_2^p\psi_1(z_{10})X_1'(z_{20})}{n_1^p\psi_1(z_{10})\psi_1'(z_{20}) - n_2^p\psi_1(z_{10})\psi_1(z_{20})} \quad (4)$$

Also, $\psi_l(z) = zJ_l(z)$ and $X_l(z) = zY_l(z)$, where J_l and Y_l are the spherical Bessel functions of first and second kind. The characteristic equation can be used to identify eigen frequencies. The geometric dispersion is the difference in resonance frequencies where $\nu_l = ck_l/2\pi n_2$ and $\Delta\nu_l = \nu_{l+1} - \nu_l$ On the other hand material dispersion is related to the Sellmeier equations[42]

$$n^2-1=\frac{B_1\lambda^2}{\lambda^2-C_1^2}+\frac{B_2\lambda^2}{\lambda^2-C_2^2}+\frac{B_3\lambda^2}{\lambda^2-C_3^2} \quad (5)$$

where n is the refractive index of the material. The constants are determined by experiments and, for silica, B_1 = 0.6961663, B_2 = 0.4079426, B_3 = 0.8974794, C_1 = 0.0684043, C_2 = 0.1162414 and C_3 = 9.896161.[42] The total dispersion is obtained by summing the geometric and material dispersion (Fig. 6). The plot shows how the ZDW can be pushed into the visible range by using thinner wall and larger bubble diameters. Theoretical calculations for materials other than silica are available in.[43]

Recently, experimental work confirmed these theoretical predictions by demonstrating, for the first time, a direct Kerr comb in the visible range.[44] 14 comb lines were observed around a pump wavelength of 765 nm (Fig. 7). The result suggests that comb lines could be pushed further into the visible range by simply decreasing the wall thickness and increasing the pump power. The table summarizes the current state-of-the-art for comb generation in hollow microresonators.

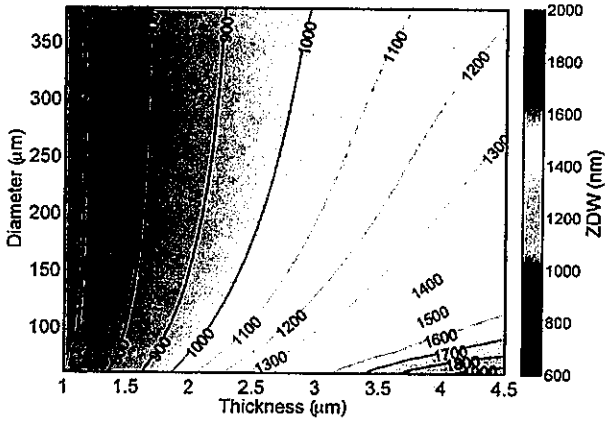

Fig. 6 Dispersion for TM modes in MBR. Reproduced with permission from. ref. 41)

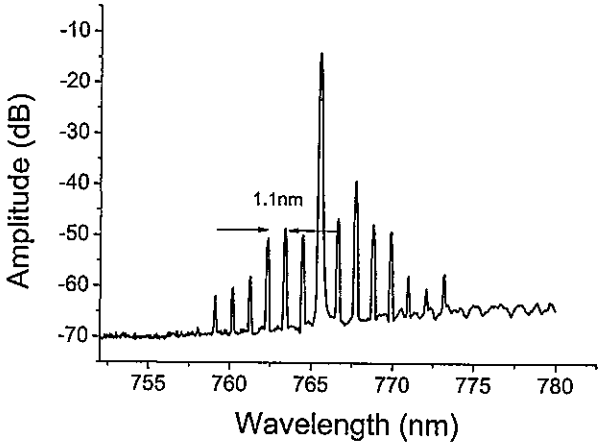

Fig. 7 Frequency comb generation in an MBR at a center wavelength of 765 nm. Up to 14 comb lines are excited. Reproduced with permission from. ref. 44)

Table 1 The current state-of-the-art of frequency comb generation in MBRs.

Team	Lei	Soria	Nic Chormaic
Diameter (μm)	136	475	120
Wall Thickness (μm)	3 – 4	3 – 4	< 1.5
Pump Wavelength (nm)	~1545	1552.4	~ 765
Laser Pow (mW)	3 – 4	~ 80	~ 6
Q factor	5×10^7	–	–
# of comb lines	5	many	14

5. Conclusion

In this brief review, we have discussed recent progress in the generation of optical frequency combs using WGMs. The geometrical properties of these devices enables the required FWM phase matching condition to be satisfied, leading to frequency comb generation. To-date, the geometrical dispersion of hollow structure WGRs has been studied in order to broaden the comb span to the visible range. Visible combs from microresonators could have applications in ground, and satellite based, astrophysical and LIDAR measurements as well as miniaturisation of rubidium and cesium atomic clocks. Further work on this topic is ongoing worldwide, in order to increase the functionality of WGRs in frequency comb applications.

Acknowledgments

This work was supported by Okinawa Institute of Science and Technology Graduate University.

References

1) M. L. Gorodetsky, A. A. Savchenkov, and V. S. Ilchenko: Opt. Lett. **21** (1996) 453.
2) V. S. Ilchenko, M. L. Gorodetsky, X. S. Yao, and L. Maleki: Opt. Lett. **26** (2001) 256.
3) T. J. Kippenberg, S. M. Spillane, and K. J. Vahala: Appl. Phys. Lett. **85** (2004) 6113.
4) J. Ward and O. Benson: Laser Photon. Rev. **5** (2011) 553.
5) A. Chiasera, Y. Dumeige, P. Fron, M. Ferrari, Y. Jestin, G. N. Conti, S. Pelli, S. Soria, and G. C. Righini: Laser Photon. Rev. **4** (2010) 457.
6) V. S. Ilchenko, A. B. Matsko, A. A. Savchenkov, and L. Maleki: J. Opt. Soc. Am. **20** (2003) 1304.
7) D. Farnesi, A. Barucci, G. C. Righini, S. Berneschi, S. Soria, and G. N. Conti: Phys. Rev. Lett. **112** (2014) 093901.
8) Y. Wu, J. M. Ward, and S. Nic. Chormaic: J. Appl. Phys. **107** (2010) 033103.
9) W. Lee, Q. Chen, X. Fan, and D. K. Yoon: Lab Chip **16** (2016) 4770.
10) K. Scholten, W. R. Collin, X. Fan, and E. T. Zellers: Nanoscale **7** (2015) 9282.
11) P. Wang, R. Madugani, H. Zhao, W. Yang, J. M. Ward, Y. Yang, G. Farrell, G. Brambilla, and S. Nic. Chormaic: IEEE Photonics Technol. Lett. **28** (2016) 2277.
12) W. Yoshiki and T. Tanabe: Opt. Express **22** (2014) 24332.
13) J. U. Frst, D. V. Strekalov, D. Elser, A. Aiello, U. L. Andersen, C. Marquardt, and G. Leuchs: Phys. Rev. Lett. **106** (2011) 113901.
14) Y. Li, J. Millen, and P. F. Barker: Opt. Express **24** (2016) 1392.
15) T. J. Kippenberg and K. J. Vahala: Science **321** (2008) 1172.
16) F. Monifi, J. Zhang, K. Zdemir, B. Peng, Y. Liu, F. Bo, F. Nori, and L. Yang: Nat. Photonics **10** (2016) 399.
17) Y. Chen: J. Phys. B: At. Mol. Opt. Phys. **46** (2013) 104001.
18) J. N. Eckstein, A. I. Ferguson, and T. W. Hnsch: Phys. Rev. Lett. **40** (1978) 847.

19) C. Gohle, T. Udem, M. Herrmann, J. Rauschenberger, R. Holzwarth, H. A. Schuessler, F. Krausz, and T. W. Hnsch: Nature **436** (2005) 234.
20) M. R. Holzwarth, T. Udem, T. W. Hnsch, J. C. Knight, W. J. Wadsworth, and P. S. J. Russell: Phys. Rev. Lett. **85** (2000) 2264.
21) T. Udem, R. Holzwarth, and T. W. Hnsch: Nature **416** (2002) 233.
22) Y. K. Chembo: Nanophotonics **5** (2016) 214.
23) P. Del'Haye, A. Schliesser, O. Arcizet, T. Wilken, R. Holzwarth, and T. J. Kippenberg: Nature **450** (2007) 1214.
24) M. H. P. Pfeier, C. Herkommer, J. Liu, H. Guo, M. Karpov, E. Lucas, M. Zervas, and T. J. Kippenberg: Optica **4** (2017) 684.
25) M. Sumetsky: Opt. Lett. **29** (2004) 8.
26) M. Li, X. Wu, L. Liu, and L. Xu: Opt. Express **21** (2013) 16908.
27) Y. Yang, J. M. Ward, and S. Nic. Chormaic: *Proc. SPIE* **8960** (2014) 89600I.
28) Y. Yang, Y. Ooka, R. M. Thompson, J. M. Ward, and S. Nic. Chormaic: Opt. Lett. **41** (2016) 575.
29) I. H. Agha, Y. Okawachi, M. Foster, J. Sharping, and A. L. Gaeta: Phys. Rev. A **76** (2007) 043837.
30) I. H. Agha, Y. Okawachi, and A. L. Gaeta: Opt. Express **17** (2009) 16209.
31) N. Riesen, S. V. Afshar, A. Franccois, and T. M. Monro: Opt. Express **23** (2015) 14784.
32) G. Lin and Y. K. Chembo: Opt. Express **23** (2015) 1594.
33) A. A. Savchenkov, A. B. Matsko, W. Liang, V. S. Ilchenko, D. Seidel, and L. Maleki: Nat. Photonics **5** (2011) 293.
34) K. T. Yang, K. Beha, D. C. Cole, X. Yi, P. Del'Haye, H. Lee, J. Li, D. Y. Oh, S. A. Diddams, S. B. Papp, *et al.*: Nat. Photonics **10** (2016) 316.
35) M. Sumetsky, Y. Dulashko, and R. S. Windeler: Opt. Lett. **35** (2010) 898.
36) S. Berneschi, D. Farnesi, F. Cosi, G. N. Conti, S. Pelli, G. C. Righini, and S. Soria: Opt. Lett. **36** (2011) 3521.
37) Y. Yang, S. Saurabh, J. M. Ward, and S. Nic. Chormaic: Opt. Express **24** (2016) 294.
38) D. Farnesi, A. Barucci, G. C. Righini, G. N. Conti, and S. Soria: Opt. Lett. **40** (2015) 4508.
39) S. Miller, K. Luke, Y. Okawachi, J. Cardenas, A. L. Gaeta, and M. Lipson: Opt. Express **22** (2014) 26517.
40) L. Wang, L. Chang, N. Volet, M. H. P. Pfeier, M. Zervas, H. Guo, T. J. Kippenberg, and J. E. Bowers: Laser Photon. Rev. **10** (2016) 631.
41) N. Riesen, W. Zhang, and T. M. Monro: Opt. Lett. **41** (2016) 1257.
42) I. H. Malitson: J. Opt. Soc. Am. **55** (1965) 1205.
43) N. Riesen, W. Zhang, and T. M. Monro: Opt. Express **24** (2016) 8832.
44) Y. Yang, X. Jiang, S. Kasumie, G. Zhao, L. Xu, J. M. Ward, L. Yang, and S. Nic. Chormaic: Opt. Lett. **41** (2016) 5266.

レーザーワード

WGM共振器 (whispering gallery mode resonators)

光共振器の一種．光はWGM共振器の赤道付近に分布し，動径方向と方位角方向に高次の振動を持つことが可能である．共振器は主にガラスで作られ，10〜100 μm程度の大きさを持つ．これにより光波長が780 nmおよび1550 nm付近の光学モードは効率よく触発され，10^7程度の高いQ値に容易に達することができる．また素材のガラスが持つ高いKerr非線形性が触発されることは光学コム技術において重要である．これに限らずWGM共振器は光子・音子相互作用，カオス理論，ソリトン生成などの研究も活発になされていて，センサー，通信技術，量子光学等への応用が可能である．（霞江 翔）